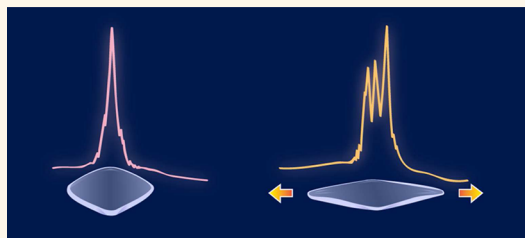


Stretchable Random Lasers with Tunable Coherent Loops

Tzu-Min Sun, Cih-Su Wang, Chi-Shiun Liao, Shih-Yao Lin, Packiyaraj Perumal, Chia-Wei Chiang, and Yang-Fang Chen*

Department of Physics, National Taiwan University, Taipei 106, Taiwan

ABSTRACT Stretchability represents a key feature for the emerging world of realistic applications in areas, including wearable gadgets, health monitors, and robotic skins. Many optical and electronic technologies that can respond to large strain deformations have been developed. Laser plays a very important role in our daily life since it was discovered, which is highly desirable for the development of stretchable devices. Herein, stretchable random lasers with tunable coherent loops are designed, fabricated, and demonstrated. To illustrate our working principle, the stretchable random laser is made possible by transferring unique ZnO nanobrushes on top of polydimethylsiloxane (PDMS) elastomer substrate. Apart from the traditional gain material of ZnO nanorods, ZnO nanobrushes were used as optical gain materials so they can serve as scattering centers and provide the Fabry–Perot cavity to enhance laser action. The stretchable PDMS substrate gives the degree of freedom to mechanically tune the coherent loops of the random laser action by changing the density of ZnO nanobrushes. It is found that the number of laser modes increases with increasing external strain applied on the PDMS substrate due to the enhanced possibility for the formation of coherent loops. The device can be stretched by up to 30% strain and subjected to more than 100 cycles without loss in laser action. The result shows a major advance for the further development of man-made smart stretchable devices.



KEYWORDS: random laser · stretchable · tunable · coherent loop · ZnO nanostructure · Fabry–Perot resonance

An emerging trend in the development offering elastic responses, such as wearable applications, human wellness, and robotic smart skins, demands advanced materials, optical and electronic devices to possess deformability.^{1–5} Stretchable laser is definitely one of the fundamental building components involving a great range of technologies, including sensors, displays, information communications and processing. The development of stretchable lasers is thus a key step toward this challenging yet exciting future. In this study, we demonstrated the stretchable random laser with tunable coherent loops based on ZnO nanomaterials deposited on polydimethylsiloxane (PDMS) elastomer substrate. Traditional lasers are composed of gain medium and optical cavities, which require precise alignment of reflective resonator cavities from meticulous fabrications,⁶ while random lasers can be obtained from gain medium and multiple scattering.^{7,8} Due to the low-cost and angle-unrestricted properties, random lasers have caught a lot of attention and have been widely applied in many kinds of aspects.^{8–10} On the other hand, the randomness of

multiple scattering keeps the random laser from easily being controlled.

ZnO is a promising ultraviolet light-emitting material due to its wide band gap (3.37 eV), high binding energy (60 meV), and excellent stability under high-temperature fabrication.^{11,12} The random laser action in ZnO powders was first observed in 1988.¹³ Since then, various kinds of ZnO nanomaterials, such as nanorods, nanoparticles, and nanowires, have been used to demonstrate random laser action based on their unique nanostructures.^{14,15} However, the controllability of the random lasers is again held back by its randomness. To take random lasers from theory to practical use, a great deal of research on tunable random lasers has been done.^{16–19} Nevertheless, most reported studies suggested that the intensity of random laser will decrease when temperature rises or the applied voltage increases, which is far from practical application. In our previous work,²⁰ we have demonstrated a selected quasi-single-mode random laser by combining ZnO nanoparticles with the skeleton of the microstructure of a butterfly wing. It is found that the selected quasi-single-mode

* Address correspondence to yfchen@phys.ntu.edu.tw.

Received for review September 15, 2015 and accepted November 8, 2015.

Published online 10.1021/acsnano.5b05814

© XXXX American Chemical Society

random laser action is achieved through the coupling between the coherent loop of random laser and Fabry–Perot resonance of the skeleton of butterfly wing. However, to our knowledge, stretchable random laser with tunable coherent loops has not yet been demonstrated. Here, by the integration of ZnO nanobrushes and PDMS elastomer film, we are able to overcome this outstanding difficulty. Unlike the most published reports,^{13–15} ZnO nanomaterials only work as scattering centers and gain media to induce random laser action; the detailed nanostructures of ZnO nanobrushes can also serve as a Fabry–Perot cavity²¹ to selectively enhance particular random laser modes. With the stretchability, the formation of coherent loops of random laser action can be manipulated by PDMS elastomer film, which enables us to reach the goal for the demonstration of stretchable random lasers with tunable coherent loops. This unique attribute adds a unique feature in the functionalities of stretchable devices and should be able to play a key step for the future development and application of this emerging field.

RESULTS AND DISCUSSION

Figure 1a shows the scanning electron microscope (SEM) image of ZnO nanobrushes with a unique structure different from the usual ZnO nanorods. The separation between each nanobrush is about 10–20 μm . In Figure 1b, the SEM image in higher resolution shows the space between the spiny rods on each nanobrush is $<1 \mu\text{m}$. The existence of ZnO was confirmed by the X-ray diffraction (XRD) image shown in Figure 2. It can be seen that all the peaks perfectly match the Zincite phase (PDF36-1451). The emission spectra of ZnO nanobrushes, excited by 266 nm pulsed laser, are shown in Figure 3, in which the broad emission peak can be attributed to band-edge transition.^{13,22,23} As the pumping energy increases, the emission intensity increases and the line width becomes narrower, which provides an indication of amplified spontaneous emission (ASE). The photoluminescence emission spectrum has a half width at half-maximum (fwhm) of about 15 nm, whereas the line width of ASE emission is narrowed down to 3 nm. The appearance of ASE provides a possibility for a random laser action to occur in ZnO nanobrushes. Indeed, random laser action appears when the pumping energy exceeds 72.1 μJ . The occurrence of random laser includes two key factors. The first factor is the gain medium, which can provide light emission under an external excitation. The second factor is the scattering medium, which can serve as the scattering center for the emitted light to form coherent loops and induce the stimulated radiation when the gain exceeds the loss. To confirm the existence of random laser action, Figure 4 shows the integrated intensity as a function of the pumping energy. In the beginning, the relationship is basically linear, but there exists a sudden change in the slope at a threshold energy of 72.1 μJ ,

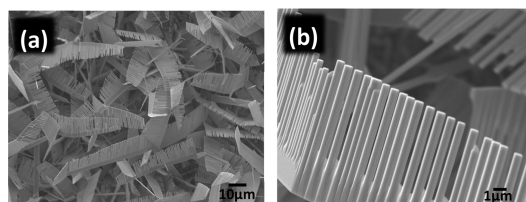


Figure 1. (a) Low-magnification and (b) high-magnification SEM images of nanobrushes.

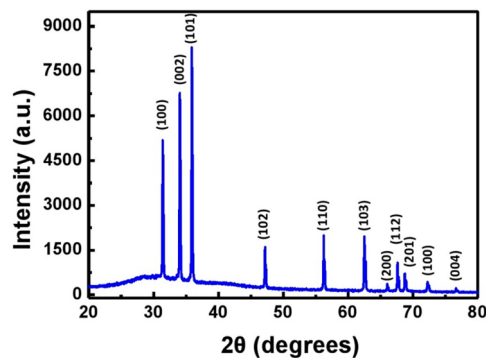


Figure 2. XRD image of ZnO nanobrushes grown by VS method.

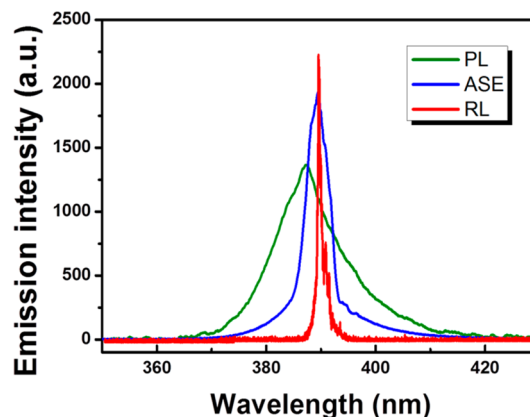


Figure 3. Photoluminescence, ASE, and random laser action of ZnO nanobrushes.

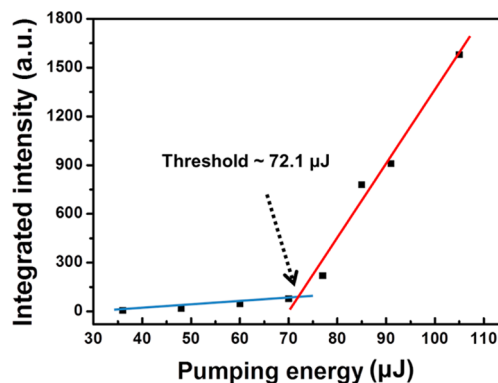


Figure 4. Integrated intensity versus pumping energy.

which provides a clear signature for the occurrence of laser action. Unlike traditional lasers, the coherent loops of random laser action are formed by the random

scattering of nanostructures, which leads the fluctuations of the position and intensity of the sharp peaks at different moments. In addition, unlike conventional lasers, the output of laser action can be detected in different angles.¹³ To confirm this unique feature, lasing spectra measured at different angles are shown in Figure 5. It is worth noting that the random laser spectra observed here with a distinct quasi-single mode are very different from a large number of multiple sharp peaks of random laser spectra detected in other ZnO nanostructures, such as nanorods.¹² For example, the different laser spectra from ZnO nanorods and ZnO nanobrushes

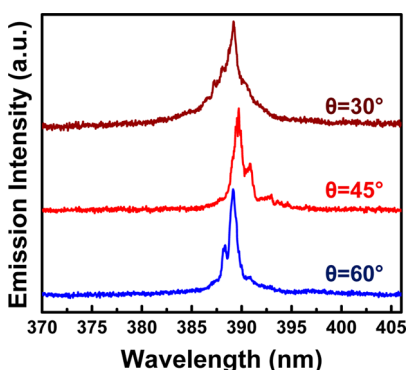


Figure 5. Spectra of random laser detected in different angle.

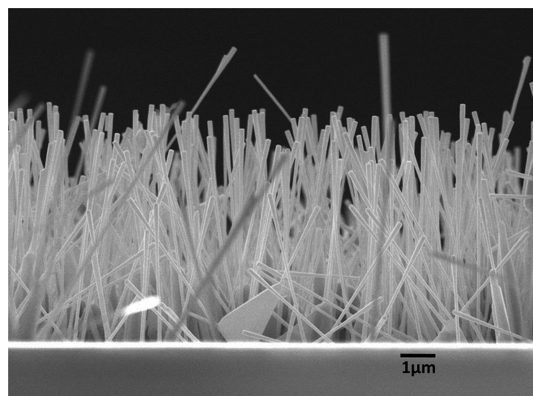


Figure 6. SEM image of ZnO nanorods.

are shown in Figure 6 for comparison. The morphology of the studied ZnO nanorods can be clearly seen by the SEM image as shown in Figure 7. Therefore, the contributing factor of the distinct quasi-single lasing peak from ZnO nanobrushes is more than the pure random laser action. The origin that multiple lasing modes from ZnO nanorods are reduced to quasi-single mode in ZnO nanobrushes is because only a specific random lasing mode with particular wavelength can be enhanced by the spiny rod of ZnO nanobrushes. More precisely, random laser action from disordered ZnO structures and Fabry–Perot resonance in spiny branches occurs simultaneously in ZnO nanobrushes resulting in an enhanced random laser action with quasi-single mode. Since there are two conditions to satisfy in forming a random laser action in ZnO nanobrushes, the enhanced laser action provides only a quasi-single high intensity peak. A more detailed discussion can be found in our previous report.²⁰ This intriguing behavior is very useful for the demonstration of tunable coherent loops by stretching as shown below.

Figure 8 shows the effect of stretching on the random laser spectra with a fixed pumping energy of 102 μJ . Figure 8a represents the sharp lasing peak of ZnO nanobrushes centered at 388.1 nm with a line width of 1.1 nm without an external strain. Figures 8b–d shows the laser spectra of ZnO nanobrushes stretched by 10%, 20%, and 30% strain, respectively. Quite interestingly, the lasing modes increase from 1, 2, and 3 to 5 as the external strain increases. It is worth mentioning that although the number of lasing mode is not completely fixed due to the nature of random lasing, the fact that lasing mode increases with increasing strain is based on the average number of the statistic result as shown in Figure 8e–h. Note that after subjecting more than 100 cycles, the device still exhibits random laser action. To understand the above interesting behavior of the stretchable random laser action, we consider the fundamental closed loop path for a random laser, which has been widely discussed before.^{13,24} To form a closed loop path, the density of the scattering centers cannot be

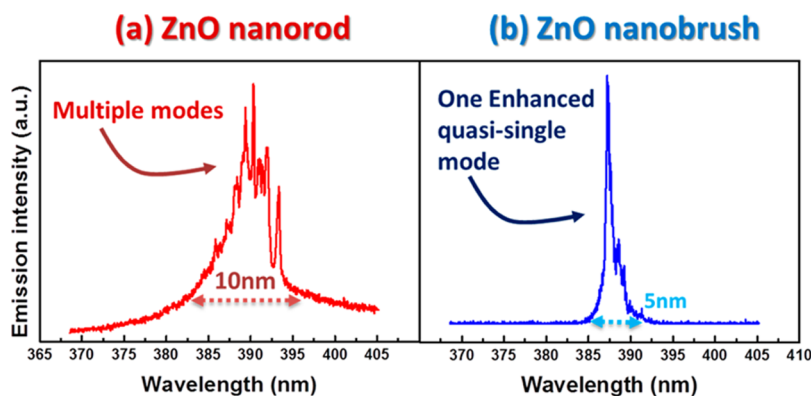


Figure 7. (a) Random laser action from ZnO nanorods. (b) Random laser action from ZnO nanobrushes without external strain.

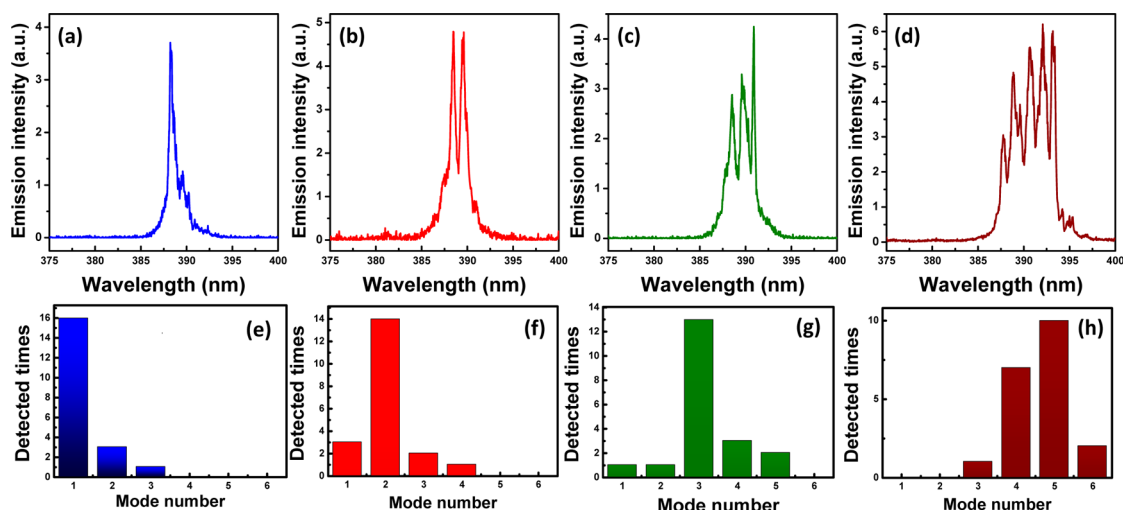


Figure 8. (a) Lasing action before stretching. Lasing action of stretching length (b) 10%, (c) 20%, and (d) 30%. (e) Detected times versus lasing mode number before stretching. Detected times versus lasing mode number of stretching length (f) 10%, (g) 20%, and (h) 30%.

too high. If the density is too high, there will not be enough room for photon to form a closed loop inside the gain medium. As shown in Figure 8a, only one lasing mode meets the condition of random laser action and Fabry–Perot resonance, simultaneously. When the PDMS elastomer substrate is stretched, the density of ZnO nanobrushes is reduced. Thus, there becomes more room for photons to travel. With more room, more closed loop paths can be formed due to multiple scattering events, which provide more enhanced lasing modes. To confirm the above proposed mechanism, we estimated the closed loop path by the following formula for laser action discussed previously:^{21,25,26}

$$2nL = M\lambda \quad (1)$$

where n is the index of refraction, L is the resonant cavity length, M is a positive integer mode number, and λ is the wavelength. From eq 1 the mode spacing can be found to be²¹

$$\frac{\Delta\lambda}{\lambda^2} = \frac{\left(n - \lambda \frac{dn}{d\lambda}\right)^{-1}}{2L} \quad (2)$$

The above equation shows that when the resonant cavity length (L) increases, the mode spacing ($\Delta\lambda$) will decrease, so the lasing peak will then increase. This predicted result is consistent with our observation. In addition, based on the mode spacing, the estimated resonant cavity length is about $10 \mu\text{m}$, which is in good agreement with the length of the spiny branch in ZnO nanobrushes. Again, this behavior further confirms the fact that the distinct sharp peaks of random laser action in ZnO nanobrushes arise from the simultaneous occurrence of the formation of coherent loops due to scattering and Fabry–Perot resonance. In short, eq 2 reveals the tendency to provide more lasing modes when the closed loop paths are enlarged.

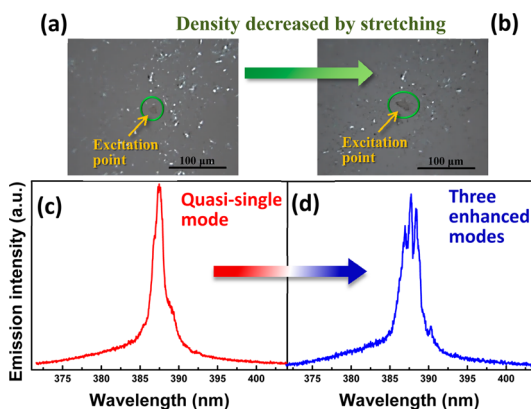


Figure 9. (a) The image of ZnO nanobrushes represented by white spots on PDMS taken by optical microscope before stretching. (b) The image of ZnO nanobrushes on PDMS taken by optical microscope after stretching. (c) The random laser action spectrum with quasi-single mode from ZnO nanobrushes before stretching. (d) The random laser action spectrum with three distinct modes from ZnO nanobrushes after stretching.

In order to verify that the increasing mode numbers arises from the change of density instead of the change of excitation point, Figure 9 shows the images of nanobrushes taken by an optical microscope and the corresponding spectra excited by 266 pulse laser under the same pumping energy of $80.5 \mu\text{J}$. In Figure 9a,b, it can be seen that the density of nanobrushes decreases after the PDMS elastomer substrate gets stretched. Also, the excitation point remains the same after the stretching process. The spectrum in Figure 9c shows a quasi-single mode random laser action. After the PDMS elastomer substrate is stretched, the mode of laser action from ZnO nanobrushes increases to three, which is shown in Figure 9d. Since the excitation point is unchanged, this experiment provides a direct evidence that the phenomenon of increasing mode can be attributed to the change of density ZnO nanobrushes.

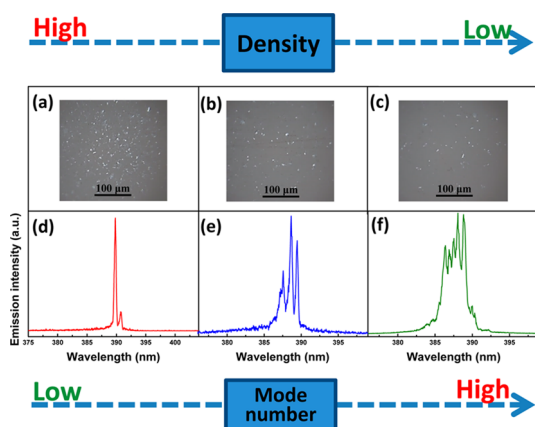


Figure 10. (a) ZnO nanobrushes transferred on PDMS with the highest density. (b) ZnO nanobrushes transferred on PDMS with a lower density. (c) ZnO nanobrushes transferred on PDMS with the lowest density. (d) The random laser action from ZnO nanobrushes with highest density. (e) The random laser action from ZnO nanobrushes with lower density. (f) The random laser action from ZnO nanobrushes with lowest density.

Moreover, in Figure 10, ZnO nanobrushes were transferred on PDMS elastomer substrate with three different densities. In the pictures, the white spots represent the ZnO nanobrushes. It can be seen that the loading fractions of the ZnO nanobrushes decrease subsequently from Figure 10a,b to c. The corresponding lasing spectra are shown in Figure 10d–f, which exhibits the fact that the number of lasing modes does increase with decreasing the density of ZnO nanobrushes. This property perfectly matches the density-dependent behavior observed by stretching.

Finally, to further confirm our proposed mechanism that the morphology of ZnO nanobrushes plays an important role for the observed laser action, we provide two kinds of ZnO nanobrushes with different spiny rod lengths. Figure 11a shows the spectrum of the first kind of ZnO nanobrushes with longer spiny rods. The SEM image in the inset of Figure 11a shows the spiny rod length of the first kind of ZnO nanobrushes is about $10\ \mu\text{m}$. Figure 11b shows the spectrum of the second kind of ZnO nanobrushes. The inset of Figure 11b shows the spiny rod length is about $8\ \mu\text{m}$, which is 20% shorter than the first one. The eq 2 of Fabry–Perot resonance shows the mode spacing ($\Delta\lambda$) is directly proportional to the inverse of the cavity length (L). The average mode spacing in Figure 11a is about 1.02 nm, and average mode spacing in Figure 11b is about 1.25 nm. This experimental result is in good agreement with the eq 2 of Fabry–Perot resonance. It provides a firm evidence to support the fact that the enhanced laser action arises from the cavity resonance of the spiny rods.

METHODS

ZnO nanobrushes were grown on silicon (Si) substrate by vapor–solid (VS) method.^{27,28} The silicon substrate ($0.5 \times 0.5\ \text{cm}$)

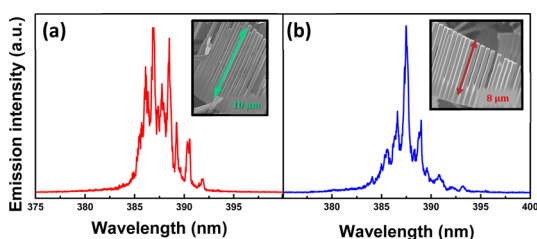


Figure 11. (a) The random laser action enhanced by longer spiny rods. Inset: the SEM image of longer spiny rods of ZnO nanobrushes. (b) The random action enhanced by shorter spiny rods. Inset: the SEM image of shorter spiny rods of ZnO nanobrushes.

It is stressed here that the unpredictable multiple modes of a random laser are usually an unfavorable property for application. However, ZnO nanobrushes emit distinct laser modes with strong intensity, and the unpredictable mode number of a conventional random laser is now turned into a controllable fashion through an external stretching. Moreover, as the number of the lasing mode increases, the spectral range of laser action increases. It means that a larger proportion of the light emission from ZnO nanobrushes will not lose its energy during the scattering process. Rather, more light emission can resonate in closed loop paths to amplify its intensity and induce laser action.

SUMMARY

In summary, we have successfully demonstrated a stretchable random laser with tunable coherent loops based on ZnO nanobrushes deposited on PDMS elastomer substrate. With the coupling between the Fabry–Perot resonance nanospiny branches on ZnO nanobrushes and the formation of closed loops due to scattering events, distinct and enhanced random laser sharp peaks can be obtained. The PDMS elastomer substrate gives an additional degree of freedom to change the space between each nanobrush. By extending the stretchable substrate, the density of ZnO nanobrushes can be reduced to an adequate magnitude for the formation of more coherent loops for random lasing to occur. Quite interestingly, as the substrate being stretched subsequently, the lasing modes gradually increase, which is consistent with our proposed mechanism that the formation of coherent closed loops increases with increasing external strain. The result shown here adds an additional feature for the functionalities of stretchable devices. In view of the importance of lasers in our daily life, it is believed that our result should be very useful and timely for the future development of stretchable devices and applications, including wearable devices, medical monitors, sensitive robotic skins, and data communication.

was ultrasonically cleaned for 10 min in acetone, ethanol, and deionized (DI) water. Zn powder was placed on one end of a ceramic boat, and the Si substrate was placed above the powder.

Then the ceramic boat was positioned to the center of a horizontal tube furnace. Subsequently, the reaction chamber was evacuated, and high-purity oxygen gas (99.9%) and argon gas (99.9%) were introduced into the reaction chamber at a flow rate of 200 and 10 sccm, respectively. The chamber pressure was about 10 Torr. After these steps, the temperature of the furnace was elevated at a rate of $60\text{ }^{\circ}\text{C min}^{-1}$ to $660\text{ }^{\circ}\text{C}$ and maintained for 60 min to grow ZnO nanobrushes. During the process, the vaporized Zn powder reacted with oxygen and turned out to be the ZnO nanobrushes. For growing ZnO nanorods, all steps are the same except the flow rate of oxygen is reduced to 5 sccm. For the stretchable elastomer substrate, PDMS solution was purchased from Dow Corning sylgard 184 and mixed with cross-linking solution with the ratio of 1:10. After the mixing process, the solution was dried at $60\text{ }^{\circ}\text{C}$ for 1 h. ZnO nanobrushes were transferred on top of PDMS elastomer substrate based on the sticky nature of the attractive force between ZnO nanobrushes and PDMS elastomer film similar to gecko tape, which can tightly bind the two contact surfaces together. Finally, the elastomer PDMS substrate deposited with ZnO nanobrushes was placed on a stage that can be stretched by a spiral micrometer.

The morphology of ZnO nanobrushes was performed by SEM (JSM-6500F). The XRD analysis was carried out using a diffractometer (Panalytical X'pert PRO). The photoluminescence spectra of ZnO nanobrushes were excited by a Q-switched Nd: YAG laser (266 nm, 3–5 ns pulse, 10 Hz). The laser beam was focused to a diameter about $300\text{ }\mu\text{m}$. The laser spectra were detected by Jobin Yvon iHR550 imaging spectrometer system. All the emission measurements were performed at room temperature.

Conflict of Interest: The authors declare no competing financial interest.

Acknowledgment. This work was supported by the Ministry of Science and Technology and the Ministry of Education of the Republic of China.

Note Added after ASAP Publication: This paper was published ASAP on 11/12/15. The spelling of the 4th author was corrected and the revised version was reposted on 11/17/15.

REFERENCES AND NOTES

- Khang, D.-Y.; Jiang, H.; Huang, Y.; Rogers, J. A. A Stretchable Form of Single-Crystal Silicon for High-Performance Electronics on Rubber Substrates. *Science* **2006**, *311*, 208–212.
- Ko, H. C.; Stoykovich, M. P.; Song, J.; Malyarchuk, V.; Choi, W. M.; Yu, C.-J.; Geddes, Iii, J. B.; Xiao, J.; Wang, S.; Huang, Y.; et al. A hemispherical electronic eye camera based on compressible silicon optoelectronics. *Nature* **2008**, *454*, 748–753.
- El-Kady, M. F.; Strong, V.; Dubin, S.; Kaner, R. B. Laser Scribing of High-Performance and Flexible Graphene-Based Electrochemical Capacitors. *Science* **2012**, *335*, 1326–1330.
- White, M. S.; Kaltenbrunner, M.; Glowacki, E. D.; Gutnichenko, K.; Kettlgruber, G.; Graz, I.; Aazou, S.; Ulbricht, C.; Egbe, D. A. M.; Miron, M. C.; et al. Ultrathin, highly flexible and stretchable PLEDs. *Nat. Photonics* **2013**, *7*, 811–816.
- Xu, S.; Zhang, Y.; Jia, L.; Mathewson, K. E.; Jang, K.-I.; Kim, J.; Fu, H.; Huang, X.; Chava, P.; Wang, R.; et al. Soft Microfluidic Assemblies of Sensors, Circuits, and Radios for the Skin. *Science* **2014**, *344*, 70–74.
- Noh, H.; Yang, J.-K.; Liew, S. F.; Rooks, M. J.; Solomon, G. S.; Cao, H. Control of Lasing in Biomimetic Structures with Short-Range Order. *Phys. Rev. Lett.* **2011**, *106*, 183901.
- Feng, S.; Kane, C.; Lee, P. A.; Stone, A. D. Correlations and Fluctuations of Coherent Wave Transmission through Disordered Media. *Phys. Rev. Lett.* **1988**, *61*, 834–837.
- Wiersma, D. S. The physics and applications of random lasers. *Nat. Phys.* **2008**, *4*, 359–367.
- Nizamoglu, S.; Gather, M. C.; Yun, S. H. Biomaterial Laser: All-Biomaterial Laser Using Vitamin and Biopolymers (Adv. Mater. 41/2013). *Adv. Mater.* **2013**, *25*, 5988–5988.
- Redding, B.; Cerjan, A.; Huang, X.; Lee, M. L.; Stone, A. D.; Choma, M. A.; Cao, H. Low spatial coherence electrically pumped semiconductor laser for speckle-free full-field imaging. *Proc. Natl. Acad. Sci. U. S. A.* **2015**, *112*, 1304–1309.
- Huang, M. H.; Wu, Y.; Feick, H.; Tran, N.; Weber, E.; Yang, P. Catalytic Growth of Zinc Oxide Nanowires by Vapor Transport. *Adv. Mater.* **2001**, *13*, 113–116.
- Djurisic, A. B.; Leung, Y. H. Optical properties of ZnO nanostructures. *Small* **2006**, *2*, 944–61.
- Cao, H.; Zhao, Y. G.; Ho, S. T.; Seelig, E. W.; Wang, Q. H.; Chang, R. P. H. Random Laser Action in Semiconductor Powder. *Phys. Rev. Lett.* **1999**, *82*, 2278–2281.
- Yu, S. F.; Yuen, C.; Lau, S. P.; Park, W. I.; Yi, G.-C. Random laser action in ZnO nanorod arrays embedded in ZnO epilayers. *Appl. Phys. Lett.* **2004**, *84*, 3241.
- Hsu, H.-C.; Wu, C.-Y.; Hsieh, W.-F. Stimulated emission and lasing of random-growth oriented ZnO nanowires. *J. Appl. Phys.* **2005**, *97*, 064315.
- Lee, C.-R.; Lin, S.-H.; Guo, J.-W.; Lin, J.-D.; Lin, H.-L.; Zheng, Y.-C.; Ma, C.-L.; Horng, C.-T.; Sun, H.-Y.; Huang, S.-Y. Electrically and thermally controllable nanoparticle random laser in a well-aligned dye-doped liquid crystal cell. *Opt. Mater. Express* **2015**, *5*, 1469.
- Chen, R.; Ta, V. D.; Sun, H. Bending-Induced Bidirectional Tuning of Whispering Gallery Mode Lasing from Flexible Polymer Fibers. *ACS Photonics* **2014**, *1*, 11–16.
- Li, L.; Wang, L.; Deng, L. Low threshold random lasing in DDPDLcs, DDPDLc@ZnO nanoparticles and dye solution@ZnO nanoparticle capillaries. *Laser Phys. Lett.* **2014**, *11*, 025201.
- Wiersma, D. S.; Cavalieri, S. Light emission: A temperature-tunable random laser. *Nature* **2001**, *414*, 708–709.
- Wang, C.-S.; Chang, T.-Y.; Lin, T.-Y.; Chen, Y.-F. Biologically inspired flexible quasi-single-mode random laser: An integration of *Pieris canidia* butterfly wing and semiconductors. *Sci. Rep.* **2014**, *4*, 6736.
- Nathan, M. I.; Fowler, A. B.; Burns, G. Oscillations in GaAs Spontaneous Emission in Fabry-Perot Cavities. *Phys. Rev. Lett.* **1963**, *11*, 152–154.
- Yoshino, K.; Tatsuhara, S.; Kawagishi, Y.; Ozaki, M.; Zakhidov, A. A.; Vardeny, Z. V. Amplified spontaneous emission and lasing in conducting polymers and fluorescent dyes in opals as photonic crystals. *Appl. Phys. Lett.* **1999**, *74*, 2590–2592.
- Cao, H.; Xu, J. Y.; Chang, S. H.; Ho, S. T. Transition from amplified spontaneous emission to laser action in strongly scattering media. *Phys. Rev. E: Stat. Phys., Plasmas, Fluids, Relat. Interdiscip. Top.* **2000**, *61*, 1985–1989.
- Bahoura, M.; Morris, K. J.; Noginov, M. A. Threshold and slope efficiency of Nd:0.5La0.5Al3(BO3)4 ceramic random laser: effect of the pumped spot size. *Opt. Commun.* **2002**, *201*, 405–411.
- Zhang, D.; Wang, Y.; Ma, D. Random lasing emission from a red fluorescent dye doped polystyrene film containing dispersed polystyrene nanoparticles. *Appl. Phys. Lett.* **2007**, *91*, 091115.
- Chen, Y. L.; Chen, C. L.; Lin, H. Y.; Chen, C. W.; Chen, Y. F.; Hung, Y.; Mou, C. Y. Enhancement of random lasing based on the composite consisting of nanospheres embedded in nanorods template. *Opt. Express* **2009**, *17*, 12706–12713.
- Sears, G. W. A growth mechanism for mercury whiskers. *Acta Metall.* **1955**, *3*, 361–366.
- Sears, G. W. A mechanism of whisker growth. *Acta Metall.* **1955**, *3*, 367–369.